Bull. Disas. Prev. Res. Inst. Kyoto Univ., Vol. 16, Part 1, No. 107, Sept., 1966

On the Mechanism of Earthquake Swarm at Hamasaka

By Yoshimichi KISHIMOTO and Michio HASHIZUME

(Manuscript received June 30, 1966)

Abstract

In June 1965 a microearthquake swarm occurred at Hamasaka, Hyogo Pref.. It was composed of about 70 shocks with two main shocks of M=3.6 and 3.1, and continued for 20 days. For the purpose of investigating the characteristics of microearthquake swarm, an analysis of this swarm was made, particularly of its fine mechannism.

The dimensions of focal domain were estimated at about several hundred meters. The magnitude distribution was very well fitted to the formula, $\log N=\alpha-\beta M$, with $\beta=0.8$. The strain energy which can be stored in this focal domain does not contradict that calculated by the formula, $\log E=11.8+1.5M$.

This swarm is separated into three sequences, bounded by two main shocks. Focal mechanisms of these earthquakes are well explained by the model of Type II. The result was derived by two methods, one being the analysis of the amplitude of initial P motion, and the other the analysis of S/P maximum amplitude ratio. Focal mechanisms in each sequence change with time. In this swarm the focal mechanism of component earthquake is considered to deviate somewhat from that of earthquakes in a stationary state in this region, but it seems to approach the stationary state at the end of each sequence. This variation of focal mechanism may have some relation to the mode of strain release.

1. Introduction

The earthquake swarm is considered an important key for clarifying the characteristics of earthquake energy and its mode of radiation, particularly when we intended to investigate earthquake mechanism by use of the microearthquakes. It is well known that, up to the present time, there have been several kinds of the mode of occurrence of the earthquake "group". The word, earthquake group, means here earthquakes which are generated in groups not only in an area but also at a time. Some groups are composed of a main shock and many subsequent shocks, while others have no conspicuously large shock but are composed of number of earthquakes. In this and the following article, we shall tentatively use the word, earthquake swarm, as a general name, including the earthquake groups of various kinds such as the main shock and subsequent shocks, and earthquake swarm in a narrow sense, and others.

Many investigations on such earthquake swarms of various magnitudes have been made, discussing, for instance, the time decay of the number of earthquakes, the magnitude distribution, the dimensions of focal domain and other matters. It seems to us, however, that these works are mainly statistical discussions of the swarm, and the treatment of the mechanism of each shock, belonging to the swarm, has been rather meager. More detailed examination of the swarm is thought necessary in order to consider its geomechanical properties.

We have frequently observed the occurrence of earthquake swarms, particu-

larly on a very small scale, in the northern Kinki District, which is covered by a network of high sensitivity seismographs, attached to the Tottori Micro-earthquake Observatory. These swarms are full of variety, not only in the number of shocks but also in their duration of activity. The smallest one is composed of perhaps only a few earthquakes and ceases within several hours, while the larger ones have hundreds of shocks continuing for a few months. Since the observation has been well done at each station of the network, these swarms are thought to offer good data for the investigation of the mechanism of earthquake swarm.

As a special instance, in June, 1965 a typical earthquake swarm occurred in the northern part of Hyogo Pref., and was well obsesved at all five stations of the network. This swarm had about 70 shocks and continued for 20 days. We shall analyse this swarm for a start, and shall apply the results in the following papers for other examples, including the Matsushiro earthquake swarm, in order to ascertain the general features of earthquake swarm.

2. Earthquake swarm at Hamasaka

This swarm occurred in June, 1965 in the northern part of Hyogo Pref.. The number of earthquakes amounted to about 70, and continued for 20 days. The epicentral region of this swarm is shown by a double circle in Fig. 1.

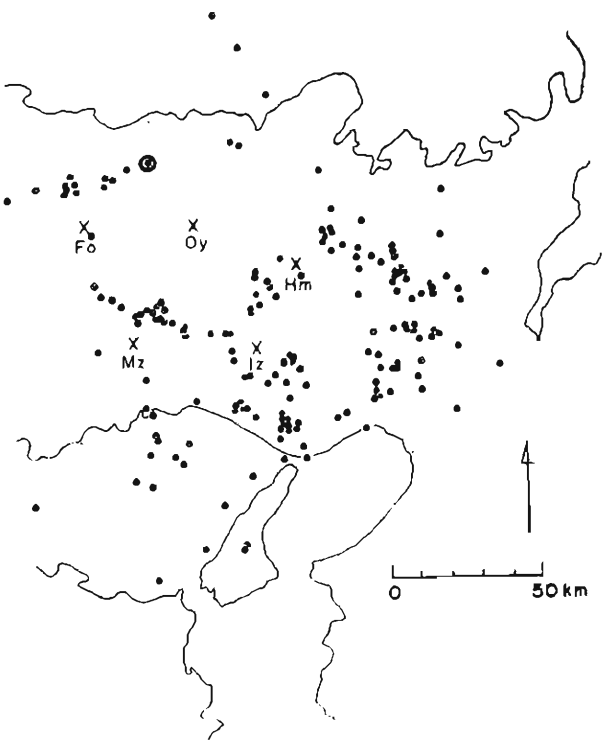

Fig. 1. Epicenter distribution. Epicenter of the swarm are shown by a double circle.

The list of these earthquakes is given in Table 1 with their magnitude, which was estimated by the method mentioned in our previous paper[1]. It seems that this swarm suddenly commenced on June 9, 1965 and ceased cmpletely on June 29, because we cannot find any trace of earthquakes in this region before June 9 or after June 29. So this swarm can be regarded as an isolated one.

A general aspect of this swarm is clearly seen in Fig. 2, in which the abscissa and ordinate show the time and the maximum velocity amplitude of vertical component observed at Hikami (HM) station, respectively. The position of the station is marked in Fig. 1.

TABLE 1.

d	h	m	M	d	h	m	M	d	h	m	M
9	06	06	0.5	16	21	58	0.9	21	04	11	1.0
10	20	23	0.9	17	09	35	1.0	21	14	17	1.4
10	20	30	1.0	17	12	29	1.0	21	17	58	2.0
10	21	49	1.5	17	17	11	0.6	21	19	02	0.8
10	22	53	0.5	18	05	10	1.5	21	19	45	1.9
11	02	50	1.8	18	06	56	1.1	21	19	51	0.5
11	14	53	0.5	18	23	18	0.5	21	20	12	0.6
13	08	23	0.5	19	05	29	0.5	21	20	40	1.0
13	09	43	1.0	19	08	47	1.1	21	21	22	0.6
14	22	42	0.6	19	13	40	0.5	21	22	21	1.5
15	09	43	0.6	20	09	13	2.8	22	05	04	2.0
15	10	22	3.3	20	06	39	0.8	22	12	39	1.5
15	11	29	1.0	20	10	13	0.5	22	14	01	0.5
15	12	44	1.2	20	15	04	0.7	24	22	57	0.7
15	04	03	1.1	20	18	16	1.0	27	00	20	2.1
16	11	49	1.5	21	00	46	0.9	28	15	11	1.5
16	17	26	1.0	21	01	25	1.1	29	07	38	1.5
16	20	30	0.9	21	01	46	1.2				
16	21	14	1.9	21	03	45	1.0				

List of earthquake swarm at Hamasaka

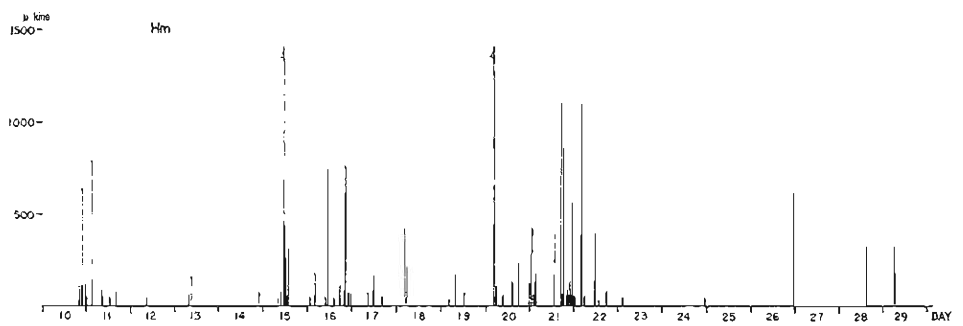

Fig. 2. Velocity amplitude of successive shocks at HM station. Two main shocks with arrowhead were off scale.

(*a*) *Epicentral region*

The epicenters of these shocks were determined by a graphical method using S-P time, which, taking the observational error into consideration, gives a most probable hypocenter. In the present case, S-P time distribution of the swarm at each station is concentrated around a certain value and it was not possible to detect the deviation of epicenter of each earthquake by this graphcal method, when we take the observational error into consideration. The epicenter and focal depth were thus estimated as shown in Fig. 1 for the epicenter, and 10 km for the focal depth for all shocks. This means that all earthquakes in this swarm occurred in a very small area, and we have therefore adopted another method to discover the dimensions of the focal domain of the swarm. Tsumura[2] has stated a method to determine the dimensions of focal domain, using the fluctuation of arrival time difference between any two stations. The same method will be used here. Let us consider the distribution of arrival time difference of P wave between any two stations. Then we take the standard deviation, δ, of this distribution and assume that δ shows the expansion of focal domain. In this method, the observational error is not allowed for, so that the focal dimensions thus derived may give the upper limit of the focal domain. The procedure is shown in Fig. 3 in which some pairs are omitted in order to avoid confusion. If we assume that the focal depth of these earthquakes are all 10 km and the above fluctuation is caused only by the horizontal expansion of the focal domain, the horizontal dimensions of the focal domain are estimated as of the order of 300m~500m. On the other hand, assumig that the fluctuation is caused only by the vertical expansion of the focal domain at the depth of 10 km, the maximum vertical dimensions is worked out as 2 km.

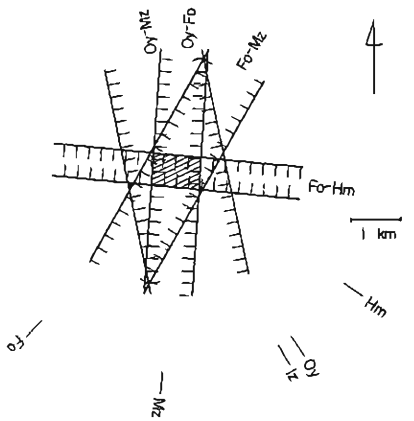

Fig. 3. Estimation of horizontal expansion of the epicentral domain.

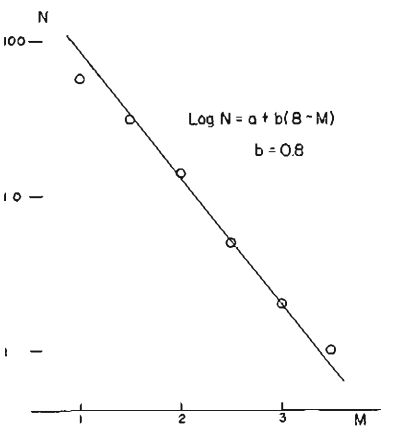

Fig. 4. Magnitude distribution.

(*b*) *Magnitude and earthquake volume*

The focal domain obtained above appears to be the so-called earthquake volume of swarm. It is interesting to calculate how much energy can be stored

in the focal domain thus estimated. The magnitude of each shock is listed in Table 1, with the two largest shocks of magnitude 3.1 and 3.6. In Fig. 4 the Gutenberg-Richter's relation between the magnitude and the number of earthquakes with corresponding magnitude, $\log N=\alpha-\beta M$, is plotted. In this case, β was obtained as 0.8, which is a very normal value in this district[3].

We shall now calculate the total energy radiated by this swarm. Since the total energy is mainly covered by the two large shocks on June 15 and 20, it is sufficient for the discussion of energy to take only these two shocks into consider ation. The sum of the energy of the two shocks is estimated by use of the formula. $\log E=11.8+1.5M$, as follows ;

for the first main shock on June 15,
$M=3.6$ $E=1.8\times10^{17}$ erg,
for the secoud main shock on June 20,
$M=3.1$ $E=3.0\times10^{16}$ erg,
total energy $E=2.1\times10^{17}$ erg.

The strain energy in unit volume of rock is, according to Tsuboi[4],

$$\varepsilon=1/2\cdot\mu x^2=2.5\times10^3\sim2\times10^4 \text{ erg.}$$

Accordingly, the earthquake volume is estimated as,

$$8\times10^{18}\sim1\times10^{13} \text{ cm}^3.$$

If we assume the epicentral area of this swarm is an ellipse, the area is calculated as follows ;

$$3.14\times150\times250\times10^4=1.1\times10^9 \text{ cm}^2.$$

Therefore the length of vertical axis of spheroid assumed as focal domain is of the order of,

140 m$\sim$1,000 m.

This value, 140 m$\sim$1,000 m, agrees approximately with that estimated by the fluctuation of arrival time difference between two stations. This results that Tsuboi's assumption of earthquake volume is valid in the present case.

3. Mechanism

It is a remarkable fact that the wave forms of earthquakes in this swarm, observed at respective stations, are very varied. Some examples of seismograms are shown in Fig. 5. As seen in this figure, the amplitude ratio of P part to S part varies from shock to shock, even at the same station. The ratio is larger than unity in some cases, while very small in others. As stated in the previous section, these earthquakes seem to have been generated in so small a region that this variety of wave form should be attributed mainly to the origin mechanism. Therefore the mechanism of this swarm will be considered in some detail in the following sections.

(*a*) *S/P maximum amplitude ratio*

To make it clear at a glance, we shall take the S/P maximum amplitude of each shock. Here the maximum amplitude of the P and S phase within 0.5 sec after the initial movement is taken, because the P and S initial wave train seems to continue about 0.5 sec after the initial motion. Fig. 6 shows the time variation of this ratio at each station, in which the vertical component is used.

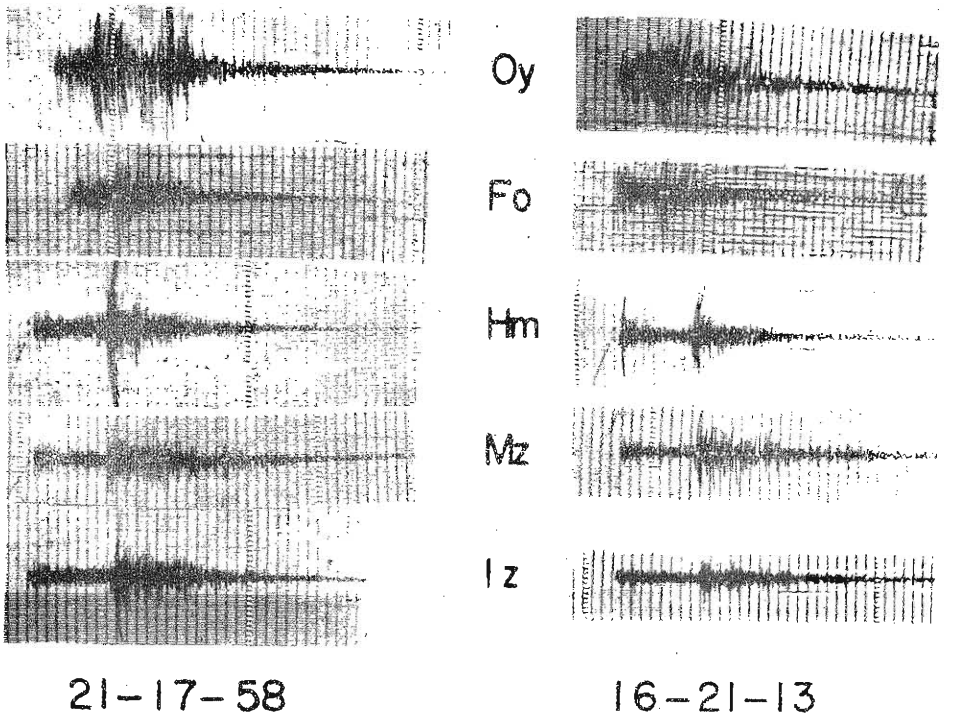

Fig. 5. Some examples of seismogram at respective stations (vertical compnent).

It is clearly seen that the time variation of the ratio is divided into three parts, between two main shocks on June 15 and 20. Moreover, the mode of time variation seems to be continuous and systematic in each part.

Separation of this swarm into three parts is considered likely from the viewpoint of strain release of earthquake swarm proposed by Benioff[5]. Fig. 7 shows the strain release curve of this swarm, and we can recognize the separation into three parts as described above. Watanabe[6] has already published an investigation on the strain release of microearthquakes. According to him there are two types in the mode of strain release. One is a beforeshock sequence going ahead of the main shock, and the other an aftershock sequence fully discussed by Benioff. In the present swarm, this classification seems approximately valid, and it may be composed of two aftershock sequences and one beforeshock sequence.

It is interesting to note that the two phenomena, the chage of S/P amplitude ratio and the strain release, have some relation to each other. Comparing Fig. 6 with Fig. 7, we see that, particularly in the third sequence, the starting time of shear stress release about 20 hours after the main shock seems to correspond to the time at which the S/P ratio has an extreme value. Such phenomenon may be ultimately related to the nature of rock fracture at the focal domain.

(b) Focal mechanism by use of P amplitude

As mentioned above, this swarm seems to have gradually changed its focal

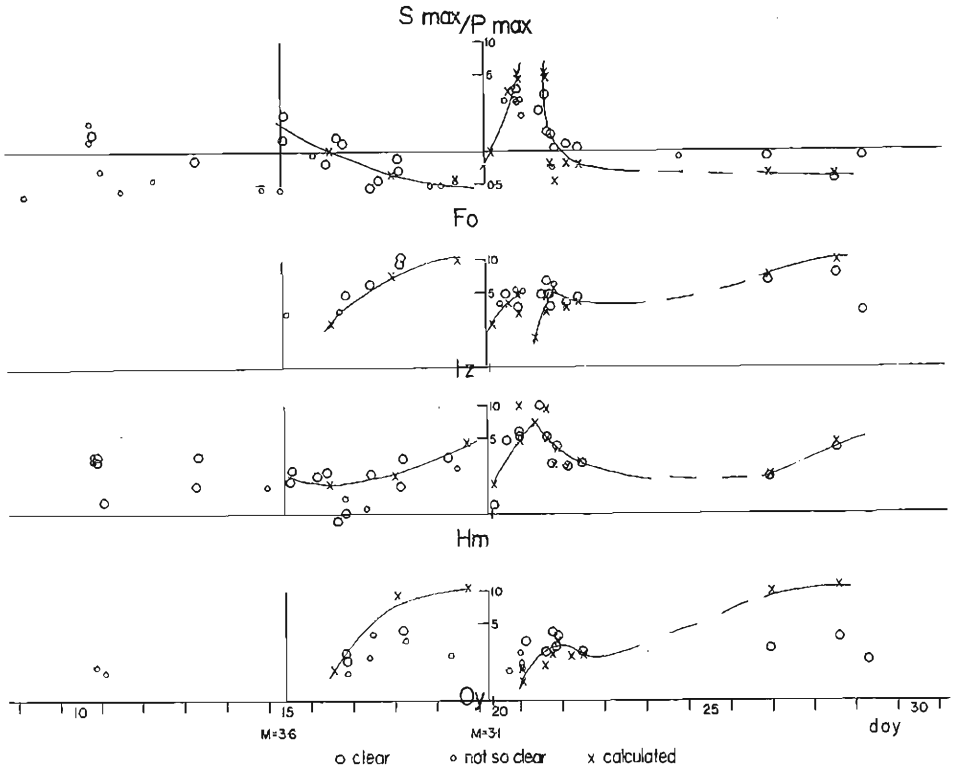

Fig. 6. Time variation of S/P maximum amplitude ratio at each station. Circles show the observed value, and cross and solid line were calculated by a procedure as described in Section 3 (c).

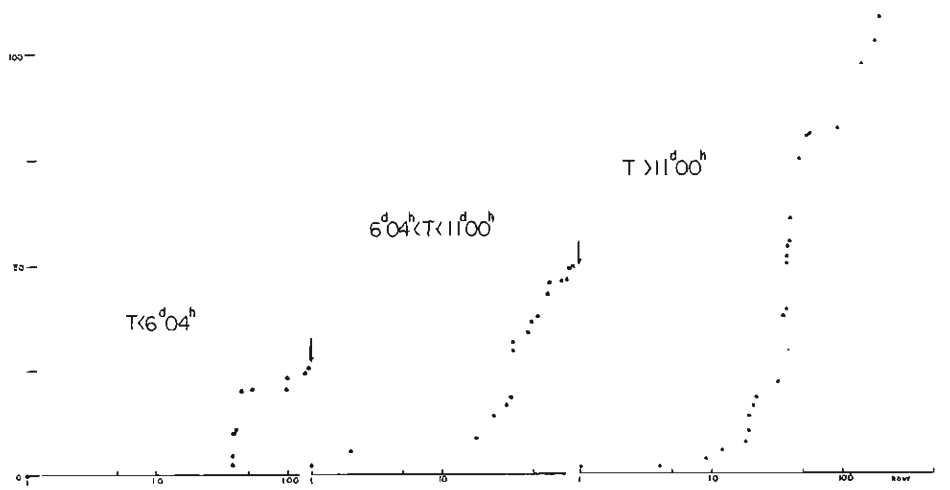

Fig. 7. Strain release curve. The arrows show the occurrence of two main shocks.

mechanism in each of three sequences. The next problem is, therefore, to find out the fine mechnism of this swarm.

It is well known that there are two prevailing model of focal mechanism, the so-called Type I and Type II. The pattern of distribution of the initial P motion is the same for both models regarding the distribution of direction and amplitude of the initial P motion. On the other hand, as regards the S wave, both models should have different patterns. Therefore, it should be possible to distinguish Type I and II, by use of the S wave. Generally speaking, however, it is difficult to idenntify the initial S motion in many cases, so that it is also difficult to decide which is more suitable, Type I or II.

We shall commence our analysis by the consideration of the amplitude itself of initial P motion, because the number of stations is so small in the present case that it is not possible to derive the mechanism of each shock by the distribution of initial P motion. Unfortunately, many shocks in this swarm were on such a small scale that the amplitude of initial P motion was too small for reliable analysis. Only in the third sequence successive shocks gave fairly good seismograms at all stations except Mikazuki(MZ), and accordingly the analysis was made particularly in the case of the third sequence.

In Table 2 the list of earthquakes used is given, in which the first column under the name of each station shows the initial P amplitude which is drawn back to the origin. Here the amplitude is normalized as 1.00 at Funaoka (FO). The hypocenters of these shocks are assumed at a depth of 10 km. The crustal structure here assumed is one stated in our previous paper[7], in which the P velocity in the first, second and third layer is 5.5, 6.1 and 6.6 km/sec, respectively, and the thickness of each layer is 3, 10 and 17 km, respectively. Therefore the hypocenters of this swarm are considered to lie in the second layer. It seems certain, by examining the time distance curve of each shock, that the initial P motion is the direct wave and not the head wave. On this assumption, in order to bring the P amplitude back to the origin some corrections were made. The attenuation of seismic wave with distance was assumed to be prortional to the reciprocal of hypocentral distance. The effect of crustal structure, namely the change of amplitude caused by reflection and refraction at each boundary surface in the crust, was corrected by the results obtained by Kawasumi and Suzuki[8]. Their calcultion was made for each boundary surface in the crustal model proposed by Matuzawa[9], in which the ratio between any two adjacent layers is $\sqrt{1.5}$ for P velocity and 1.1 for density, and the Poisson's ratio is 1/4 in all layers. Since we are concerned here with the normalized amplitude, the change caused by a little difference in the structure will not have a very serious effect. As we are now progressing in the investigation of the crustal structure in this area, this problem will be reconsidered in the future. Thus, we assumed that the amplitude ratio of the wave incident to the earth's surface to that emitted from the origin is 0.8 for FO and OY, and 0.3 for MZ, IZ and HM, for P wave. The effect of reflection at the earth's surface was assumed the same for all stations.

As described already in our previous paper[10], the distribution of the initial P motion is represented by the so-called four-quadrant type with two mutually perpendicular nodal lines intersecting at the epicenter, and with its principal pressure

acting approximately to E-W direction for almost all areas in the north-western Kinki District. The area with which we are concerned here is nearly the same, except that the direction of principal pressure deviates a little clockwise from an E-W directions. As two nodal planes are thus nearly vertical for most earthquakes in this district, we shall first assume Type II and calculate the amplitude of initial P motion for various locations of nodal planes, starting from that with two vertical nodal planes. As seen in Table 2, FO (and MZ) always give a push motion (+), and HM always a pull motion (−) of P. On the other hand, at OY and IZ push and pull motions are mixed. These facts clearly show that one nodal plane always passes through somewhere very close to OY. Thus we may take into consideration only the locations of two nodal planes, one of which necessarily passes through somewhere very close to OY. In all, 125 cases were calculated, which were, starting from the initial location, successively changed by some small angles as to ϕ, θ and ψ shown in Fig. 8. In this figure, ϕ is the azimuth of Y axis measured clockwise from E direction. As to any one position of Y axis, OQ is rotated by θ from OY to OY′ around the X axis, and finally OB rotated by ψ from OX to OX′ around OY′. Here the increment of angle is taken 5 degrees for ϕ and 10 degrees for θ and ψ. Calculations were made by the use of the formulas derived by Mikumo[11].

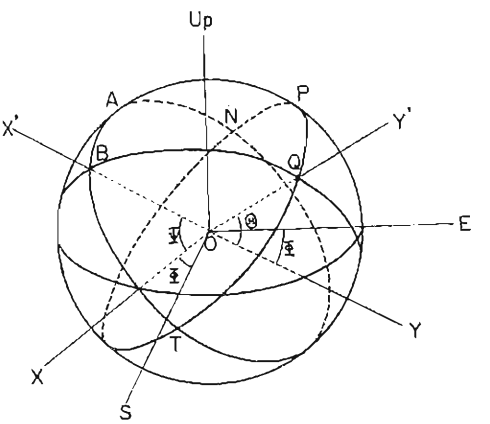

Fig. 8. Focal sphere. The great circles NABT and NPQT are two nodal planes.

125 sets of calculated values were compared with the ones observed, all being normalized, and a location which gives the least mean square root of O−C was assumed to show the focal mechanism of each shock. These results are listed in the parenthesis in Table 2, with corresponding ϕ, θ and ψ of the nodal planes. In some cases, the solution which gives the least mean square root was restricted to only one location and had fairly small residuals. But in some other cases a decision as to the most probable solution was not so easy, having a few locations with the mean square root of the some other, or the agreement of calculated value with the one observed not being so good. Generally speaking, however, a certain tendency of change of focal mechanism with time is recognized, and this tendency is in agreement with that inferred from the pattern of push-pull distribution of initial P motion in Table 2. This tendency will be mentioned again in the following section.

(c) *Use of S/P ratio*

These shocks are of such small magnitude that the initial motion cannot be reliably determined even for P wave in many shocks. Identification of the initial motion of S wave was also impossible in almost all shocks, although the arrival

TABLE 2.

d	h	m	M	FO	MZ	IZ	OY	HM	Φ	Θ	Ψ	φ	θ
21	01	46	1.5	1.00	—	2.94 (3.13)	0 (0.48)	−1.47 (−1.64)	47°	10°	−30°	3°	28°
21	17	58	2.3	1.00	—	5.94 (2.92)	0.40 (1.12)	−6.43 (−5.86)	52	−20	0	5	−14
21	19	45	2.2	1.00	—	0 (0.11)	−0.03 (−0.57)	−3.17 (−2.90)	57	−10	−10	13	0
21	22	21	1.8	1.00	—	1.00 (0.99)	0.15 (0.43)	−2.00 (−2.00)	52	0	0	7	0
22	05	04	2.3	1.00	—	0.83 (1.28)	0.08 (0.04)	−2.54 (−2.19)	52	0	−10	8	9
22	12	39	1.8	1.00	—	0.42 (0.26)	−0.04 (−0.07)	−1.76 (−1.62)	57	0	0	12	0
27	00	21	2.4	1.00	4.15 (1.37)	0.19 (0.16)	−0.03 (−0.05)	−0.32 (−1.00)	57	20	0	10	14
28	15	11	1.8	1.00	2.61 (1.95)	0.29 (0.69)	−0.03 (−0.33)	−0.20 (−0.73)	62	20	−40	15	42
29	07	38	1.8	1.00	3.25 (1.11)	−0.40 (−0.22)	−0.11 (−0.27)	−1.80 (−1.18)	62	20	10	18	7

Origin mechanism derived from the analysis of P amplitude. Φ, Θ and Ψ, θ and φ are referred to the article.

TABLE 3.

d	h	m	M	FO	MZ	1Z	OY	HM	Φ	Θ	Ψ	φ	θ
20	18	16	1.3	2.9 (3.0)	—	5.0 (4.6)	—	4.8 (4.6)	52	− 5	20	8	−18
21	01	46	1.2	3.7 (4.8)	—	3.6 (4.8)	2.2 (2.0)	5.8 (9.7)	52	−10	25	7	−24
	(*)								52	−20	20	3	−27
21	17	58	2.3	3.3 (5.4)	—	6.2 (3.5)	(1.6)	5.0 (5.2)	52	−10	25	7	−24
21	19	45	2.2	1.5 (0.8)	—	4.9 (4.2)	4.2 (2.7)	2.8 (3.0)	52	0	15	8	−10
21	22	21	1.8	1.1 (0.6)	—	6.0 (5.7)	3.8 (3.4)	4.1 (4.0)	52	0	20	9	−13
22	05	04	2.3	1.2 (0.8)	—	4.5 (4.2)	—	2.7 (3.0)	52	0	15	8	−10
22	12	39	1.8	1.1 (0.8)	—	4.6 (4.2)	2.8 (2.7)	3.0 (3.0)	52	0	15	8	−10
27	00	21	2.4	0.9 (0.6)	0.6 (0.9)	6.5 (7.2)	3.0 (10.0)	2.3 (2.3)	57	10	−15	11	8
28	15	11	1.8	0.5 (0.6)	0.9 (1.0)	7.3 (10.0)	3.7 (11.4)	4.1 (4.5)	62	20	−25	13	22
29	07	38	1.8	0.9 (—)	1.1 (—)	3.2 (—)	2.3 (—)	—	—	—	—	—	—

Origin mechanism derived from the anasysis of S/P maximum amplitude ratio. Φ, Θ and Ψ, θ and φ are referred to the article.

time of S wave was possible to determine with the accuracy of 0.1 sec. On the other hand, the fact that the time variation of S/P maximum amplitude ratio is remarkable and systematic may suggest that the focal mechanism changed gradually with time, as mentioned earlier. If, therefore, we can use the S/P maximum amplitude ratio for determination of focal mechanism, it will be very advantageous for the present discussion. S/P maximum amplitude ratio does not, of course, strictly correspond to the ratio of initial P and S motions, as derived from the theories of Type I or II. Nevertheless, we shall tentatively assume the observed S/P maximum amplitude ratio is approximately equal to the ratio of the initial P and S motions, and try a comparison of the observed ratio with the calculated one. If the same solution will be obtained as that derived from P wave in the previous section, this assumption may be approximately allowable. This assumption also may be justified to some extent by the

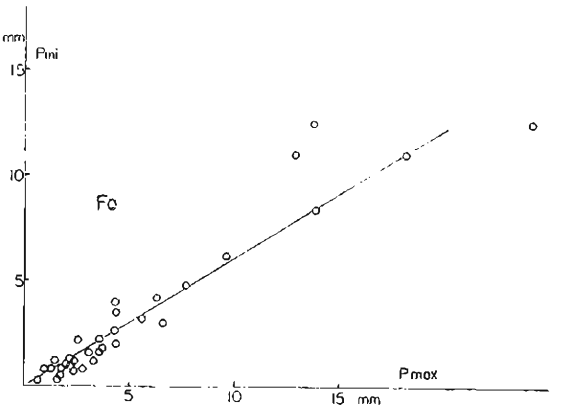

Fig. 9. Relation between the initial and maximum P amplitude at FO.

following fact. Fig. 9 shows a relation between the initial and maximum amplitude of P wave observed at FO station, where the initial P motion was clearly read in many shocks in this swarm. The plotted points are fairly well fitted to a straight line, and the maximum amplitude is approximately twice the initial motion.

We shall now look for the most preferable location of nodal planes in the same manner as described in the treatment of P wave. Table 3 shows the results for Type II, the expressions of this table being the same as in Table 2. In the present analysis, the angle of incidence at the surface is about 60°, larger than the critical, and so that the ground motion due to S wave is rather complicated. But the polarization of particle motion is not considered but only the absolute value is treated, because we are concerned here only with the maximum ampitude. It will be seen in Table 3 that the most preferable location of nodal planes is generally very close to that derived from P wave, and moreover the agreement between the observed and calculated ratio is fairly close, as seen in the table. On the other hand, the observed ratio does not agree with the

one calculated in the case of Type I. From these results, we may say that it is allowable to use the S/P maximum amplitude ratio for the estimation of focal mechanism, and also Type II seems more preferable for the shocks in the present swarm.

Fig. 10 shows graphically the focal mechanism of earthquakes in Tables 2 and 3. In this figure, the focal mechanism is represented by the direction of the principal pressure, φ and θ, which are measured in such a way as shown by a small figure inserted in the figure. We can recognize in this figure not only the agreement of both results derived form P and S/P but also nearly the same tendency of the change of focal mechanism.

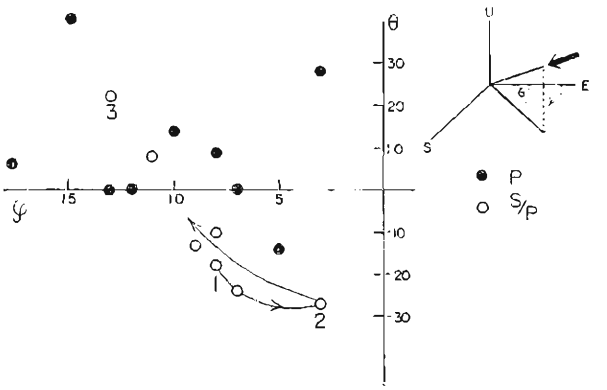

Fig. 10. Change of focal mechanism with time, represented by the direction of principal pressure (φ, θ). Point 1 and 3 correspond to the shocks at 20th 18h 16m and 28th 15h 11m. Point 2 is an extreme value estimated by the S/P curve in Fig. 6, corresponding to (*) in Table 3.

(d) Some discussions on the mechanism

As the validity of S/P maximum amplitude ratio as a method of determining the focal mechanism has been approximately ascertained, we can estimate the focal mechanism of earthquakes in which the P initial motion cannot be identified reliably. Then, connecting these results as smoothly as possible, we may infer the time variation. Such a procedure is represented by the cross mark and the solid line in Fig. 6 as to each station.

Fig. 10, presented in the previous section, means that the time variation of S/P maximum amplitude ratio corresponds to the change of focal mechanism, represented in this figure by the direction of principal pressure. The movement of plotted points from the lower right towards the upper left corresponds, for example at FO, to the decrease of S/P ratio. Accordingly the curve in each sequence in Fig. 6 may correspond to some systematic change of focal mechanism. In the previous section, 3 (a), the correspondence between the time variation of S/P ratio and the strain release curve was given. Now, since the variation of S/P ratio is assumed to show the change of focal mechanism, the strain

release may have some relation to change of focal mechanism, too. Comparing Fig. 6 with Fig. 7, we can say that, particularly in the third sequence, the tendency of change of focal mechanism may be reverse in both compressional and shear strain release. This circumstance is shown in two parts, the point I to II, and 2 to 3 in Fig. 10.

Such variation of focal mechanism does not seem to be caused by the movement of hypocenter of successive earthquakes in the sequence. If this were the case, we should observe the variation of arrival time difference between any two stations. But we cannot recognize such changes of arrival time difference, as seen in Fig. 11.

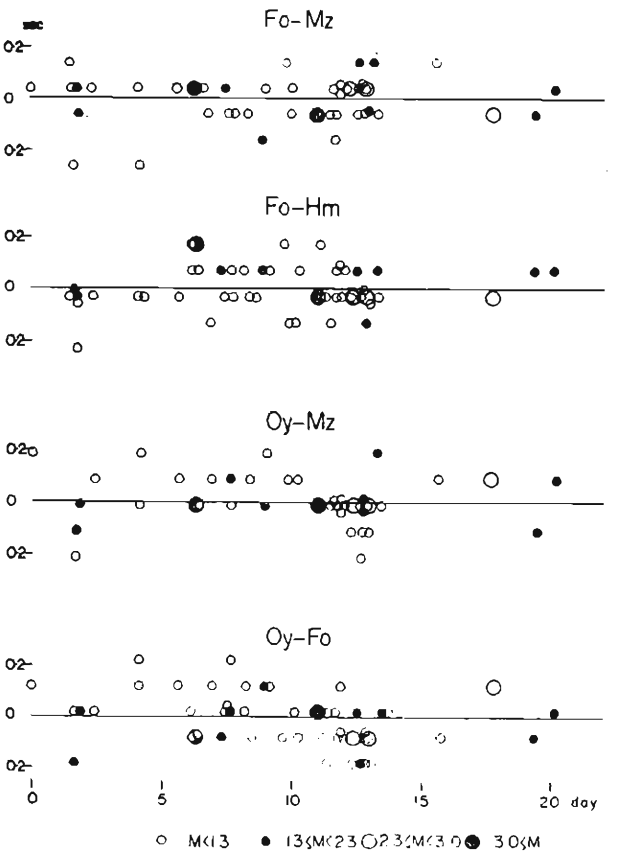

Fig. 11. Time variation of arrival time difference between two stations.

We shall reconsider the time variation of focal mechanism from the viewpoint of nodal line observed at the surface of the earth. In Fig. 12 one nodal line, passing through somewhere near OY, is drown in three cases 1, 2 and 3, corresponding to Fig. 10. The nodal line attached by a letter S is the mean nodal line of earthquakes which had been generated in this region for 10 months before June 1965[12].

In other words, nodal line, S, may represent the mechanism of earthquakes in a stationary state in this region. As described in our previous paper[13], the direction of the nodal line or the principal pressure in this stationary state in this region deviates about 30° clockwise from those of other regions, and moreover that the direction of nodal line or principal pressure of the swarm gradually approaches the stationary state. This approach to the stationary state seems to exist in other sequences as well as the third sequence mentioned above. Namely, referring to Fig. 6, the S/P ratio seems to approach the same value at the end of each sequence. If this phenomenon is real, it may be an interesting characteristic of the swarm.

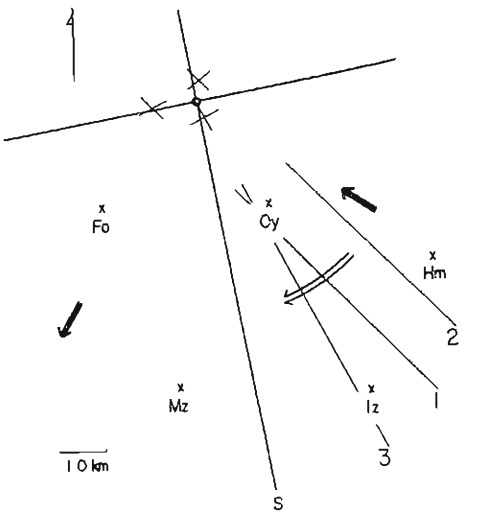

Fig. 12. Time variation of one nodal line. Lines 1, 2 and 3 correspond to points 1, 2 and 3 in Fig. 10, respectively. A nodal line with the letter S is that of earthquakes in the stationary state in this region.

There may be two important problems which should be further investigated. One is to examine whether these properties of earthquake swarm are also observable in many other cases. The other is to clarify the relation between the mechanism of earthquake swarm and that of earthquakes in a stationary state, which are thought to be generated by a certain force continuously acting over a wider area. After these investigations, we shall be able to advance to geomechanical consideration of the earthquake swarm and also general properties of seismic activity.

Acknowledgment

The authors' thanks are due to Dr. T. Mikumo and Mr. K. Oike for their valuable discussions on this problem. The authors are also very indebted to Mr. S. Yabe, Mrs. M. Koga, Miss M. Uyeda, Miss T. Hagura and Miss E. Hirai for their kind help in reading of seimograms and calculation.

References

1) Hashizume, M., K. Oike and Y. Kishimoto : Investigation of Microearthquakes in Kinki District —Seismicity and mechanism of their occurrence—, Bull. Dis. Pre. Res. Inst., Vol. 51, 1966, 35.
2) Tsumura, K. : Read at the meeting of Seismological Society of Japan, 1965.
3) Miyamura, S. ; Seismicity and geotectonics, Zisin, Vol. 15, 1962, 23. (in Japanese)
4) Tsuboi, C. ; Earthquake energy, earthquake volume, aftershock area and strength of the earth's crust, Journ. Phys. Earth, Vol. 4, 1956, 63.
5) Benioff, H. ; Earthquake and rock creep, Bull. Seism. Soc. Amer., Vol. 41, 1951, 31.
6) Watanabe, H. ; On the sequence of earthquakes, Special Contr., Geophys. Inst., Kyoto Univ., No. 4, 1964, 153.

7) Kishimoto, Y., M. Hashizume and K. Oike ; On the seismicity of microearthquakes in the western Kinki District. Disast. Prev. Res. Inst. Annuals, No. 9, 1966, 27. (in Japanese)
8) Kawasumi, H. and T. Suzuki ; Reflection and refraction of seismic waves at the interfaces in the crust, Zisin, Vol. 4, 1932, 277. (in Japanese)
9) Matuzawa, T. ; On the relative magnitude of the preliminary and the principal motion of earthquake motions, Jap. Journ. Astr. and Geophys., No. 4, 1962, 1.
10) loc. cit. 1)
11) Mikumo, T. ; Mechanism of local earthquakes in Kwanto Region, Japan, derived from the amplitude relation of P and S waves, Bull. Earthg. Res. Inst., Vol. 40, 1962, 399.
12) loc. cit. 1)
13) loc. cit. 1)